

THE MOST LUMINOUS SUPERNOVAE

TUGULDUR SUKHBOLD¹ AND S. E. WOOSLEY¹
 (Accepted —, 2016)
 15 Feb, 2016

ABSTRACT

Recent observations have revealed a stunning diversity of extremely luminous supernovae, seemingly increasing in radiant energy without bound. We consider simple approximate limits for what existing models can provide for the peak luminosity and total radiated energy for non-relativistic, isotropic stellar explosions. The brightest possible supernova is a Type I explosion powered by a sub-millisecond magnetar with field strength $B \sim \text{few} \times 10^{13}$ G. In extreme cases, such models might reach a peak luminosity of 2×10^{46} erg s⁻¹ and radiate a total energy of up to 4×10^{52} erg. Other less luminous models are also explored, including prompt hyper-energetic explosions in red supergiants, pulsational-pair instability supernovae, pair-instability supernovae and colliding shells. Approximate analytic expressions and limits are given for each case. Excluding magnetars, the peak luminosity is near 3×10^{44} erg s⁻¹ for the brightest models and the corresponding limit on total radiated energy is 3×10^{51} erg. Barring new physics, supernovae with a light output over 3×10^{51} erg must be rotationally powered, either during the explosion itself or after, the most obvious candidate being a rapidly rotating magnetar. A magnetar-based model for the recent transient event, ASASSN-15lh is presented that strains, but does not exceed the limits of what the model can provide.

Subject headings: stars: supernovae: general

1. INTRODUCTION

Motivated by the recent discovery of many ultra-luminous supernovae (ULSN), including, controversially, the extreme case of ASASSN-15lh (Dong et al. 2016; Brown 2015), the limits of several scenarios often invoked for their interpretation are considered. These include colliding shells, pair-instability supernovae, and newly-born magnetars (e.g. Gal-Yam 2012; Quimby et al. 2011). Each of these energy sources will give different results when occurring in a stripped core of helium or carbon and oxygen (Type I) or a supergiant (Type II), and both cases are considered. All calculations of explosions and light curves use the 1D implicit hydrodynamics code KEPLER (Weaver et al. 1978; Woosley et al. 2002), and employ presupernova models that have been published previously.

The more extreme case of “relativistic supernovae” - either supernovae with relativistic jets or the explosion of super-massive stars that collapse because of general relativistic instability (Fuller et al. 1986; Chen et al. 2014) is not considered here. These are rare events with their own distinguishing characteristics.

2. PROMPT EXPLOSIONS AND PAIR-INSTABILITY

Any explosive energy that deposits before the ejecta significantly expands will suffer severe adiabatic degradation that will prevent the supernova from being particularly bright. An upper bound for prompt energy deposition in a purely neutrino-powered explosion is $\sim 2 - 3 \times 10^{51}$ erg (Fryer & Kalogera 2001; Ugliano et al. 2012; Pejcha & Thompson 2015; Ertl et al. 2016), which is capable of explaining common supernovae (Sukhbold et al. 2015), but not the more luminous ones. In a red, or worse, blue supergiant, the expansion from an initial stel-

lar radius of, at most, 10^{14} cm, to a few times 10^{15} cm, where recombination occurs, degrades the total electromagnetic energy available to $\lesssim 10^{50}$ erg. Even in the most extreme hypothetical case, where a substantial fraction of a neutron star binding energy, $\sim 10^{53}$ erg, deposits instantly, the light curve is limited to a peak brightness of approximately 10^{44} erg s⁻¹ (neglecting the very brief phase of shock break out).

This can be demonstrated analytically and numerically. Adopting the expression for plateau luminosity and duration from Popov (1993) and Kasen & Woosley (2009), as calibrated to numerical models by Sukhbold et al. (2015), Type II supernovae have a luminosity on their plateaus of

$$L_p = 8.5 \times 10^{43} R_{0,500}^{2/3} M_{\text{env},10}^{-1/2} E_{53}^{5/6} \text{ erg s}^{-1}, \quad (1)$$

where $R_{0,500}$ is the progenitor radius in $500 R_{\odot}$, $M_{\text{env},10}$ is the envelope mass in $10 M_{\odot}$, and $E_{53} \lesssim 1$ is the prompt explosion energy in units of 10^{53} erg. The approximate duration of the plateau, ignoring the effects of radioactivity, is given by

$$\tau_p = 41 E_{53}^{-1/6} M_{10}^{1/2} R_{0,500}^{1/6} \text{ days}. \quad (2)$$

This plateau duration is significantly shorter than common supernovae due to the much higher energies considered.

These relations compare favorably with a model for a $15 M_{\odot}$ explosion calculated with an assumed explosion energy of 0.5×10^{53} erg (Fig. 1). Here the red supergiant presupernova stellar model from Woosley et al. (2007) had a radius of $830 R_{\odot}$ and an envelope mass, $8.5 M_{\odot}$. The estimated luminosity on the plateau from eq. (1) is 6.7×10^{43} erg s⁻¹ and duration from eq. (2) is 46 days. The corresponding KEPLER model in Fig. 1 had a duration of ~ 45 days and a luminosity at day 25 of 6.6×10^{43} erg s⁻¹. The total energy emitted is approximately

¹Department of Astronomy and Astrophysics, University of California, Santa Cruz, CA 95064. sukhbold@ucolick.org

$L_p \tau_p$, or $3 \times 10^{50} E_{53}^{2/3} R_{0,500}^{5/6}$ erg.

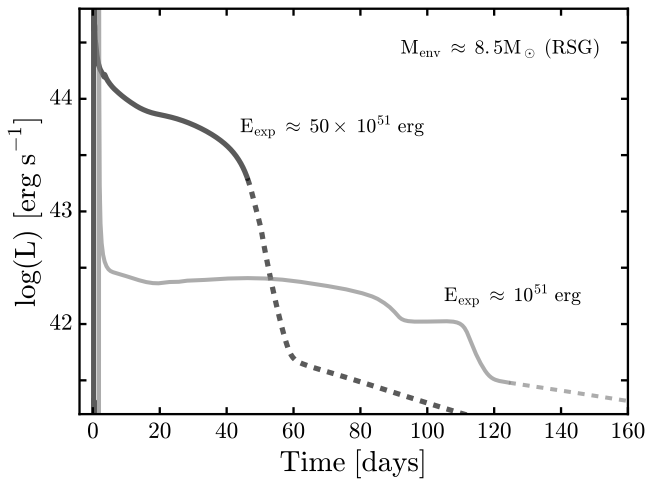


FIG. 1.— Bolometric light curves for a $15 M_{\odot}$ supergiant exploded with two different values of prompt energy deposition. One with $E_{\text{exp}} = 10^{51}$ erg, is typical of common Type IIp supernovae; the other with $E_{\text{exp}} = 50 \times 10^{51}$ erg is near the upper bound of what any prompt, point explosion might provide. Even for this extreme case, the plateau luminosity does not exceed $\sim 10^{44}$ erg s^{-1} . The curves are dashed when the ejecta become optically thin and the blackbody representation of their emission becomes questionable. The presupernova star, originally $15 M_{\odot}$ at birth, had a mass of $12.6 M_{\odot}$, of which $8.5 M_{\odot}$ was in the hydrogen envelope, and a radius of $R_{0,500} \sim 1.7$. The luminosity at shock break out in the more energetic model peaked at 1.5×10^{47} erg s^{-1} , but only lasted for about 100 seconds.

Similar limits apply to pair-instability supernovae (PISN) in red supergiant progenitors. Again, maximum explosion energies are $\lesssim 10^{53}$ erg (Heger & Woosley 2002). For the most extreme, rarest case, $M_{10} \approx 20$, $R_{0,500} \approx 5$ and $E_{53} \approx 1$, eq. (1) and eq. (2) imply plateau luminosities near 5×10^{43} erg s^{-1} for about 200 days. These values are consistent with the KEPLER models given in Scannapieco et al. (2005). The total radiated energy is 1×10^{51} erg. Most of the radioactivity decays during the plateau. Since the decay energy is substantially less than the explosion energy, the modification of the light curve during its bright plateau is not appreciable.

We conclude that ULSN must be energized by a power source that deposits its energy well after the original explosion. The known delayed energy sources are radioactivity, colliding winds, and pulsars.

3. RADIOACTIVITY

The most prolific sources of ^{56}Ni are PISN. The rarest, most massive PISN produces, at most, $50 M_{\odot}$ of ^{56}Ni in an explosion with a final kinetic energy of 9×10^{52} erg (Heger & Woosley 2002). This large production only occurs for the the most massive helium cores ($\sim 130 M_{\odot}$), which very nearly collapse to black holes. The total energy available from the decay of large amount of ^{56}Ni is substantial,

$$E_{\text{dec}} \approx 2.4 \times 10^{51} \left(\frac{M_{\text{Ni}}}{50 M_{\odot}} \right) (3e^{-t/\tau_{\text{Co}}} + e^{-t/\tau_{\text{Ni}}}) \text{ erg}, \quad (3)$$

where M_{Ni} is the ^{56}Ni mass in M_{\odot} , and $\tau_{\text{Co}} = 111$ d and $\tau_{\text{Ni}} = 8.7$ d are mean lives of ^{56}Co and ^{56}Ni . For a nickel

mass of $\sim 50 M_{\odot}$ the total energy is nearly 10^{52} erg. Most of this energy is lost during the adiabatic expansion to peak, however.

For a star that has lost its hydrogen envelope, an approximate estimate when the PISN light curve peaks is given by equating the effective diffusion timescale, t_d , to age. This gives a time of peak luminosity, t_p , of

$$t_p = \left(\frac{3\kappa}{4\pi c} \right)^{1/2} \left(\frac{M_{\text{ej}}^3}{2E_{\text{exp}}} \right)^{1/4} \\ \sim 177 \left(\frac{M_{\text{ej}}}{130 M_{\odot}} \right)^{3/4} \left(\frac{E_{\text{exp}}}{10^{53} \text{ erg}} \right)^{-1/4} \text{ days}, \quad (4)$$

where M_{ej} is the ejecta mass in M_{\odot} and E_{exp} is the explosion energy in erg. Considering the similarity of high velocity and iron-rich composition to Type Ia supernovae, an opacity $\kappa \approx 0.1 \text{ cm}^2 \text{ g}^{-1}$ is assumed. Arnett's Rule (Arnett 1979) then implies a maximum luminosity of

$$L_p \approx 8 \times 10^{44} \left(\frac{M_{\text{Ni}}}{50 M_{\odot}} \right) e^{-t_p/\tau_{\text{Co}}} \text{ erg } s^{-1}. \quad (5)$$

Only the luminosity due to the decay of ^{56}Co is included here, since for $t \sim t_p$, most of ^{56}Ni will have already decayed. For the fiducial values of t_p and M_{Ni} , the peak luminosity is then roughly 1.5×10^{44} erg s^{-1} , which compares favourably with models in which the hydrodynamics and radiation transport are treated carefully (Kasen et al. 2011; Kozyreva & Blinnikov 2015) and with the analytic models of (Chatzopoulos et al. 2013).

Assuming that the total emitted energy by a Type I supernova is

$$E_{\text{rad}} \approx \frac{1}{2} L_p t_p + E_{\text{dec}}(t_p), \quad (6)$$

and using the fiducial values, the approximate upper bound on the total luminous energy in a PISN-Type I is 2.6×10^{51} erg, about one quarter of the total decay energy.

4. COLLIDING SHELLS

4.1. Generic Models

Observations show that a substantial fraction of ULSN, especially those of Type IIIn, are brightened by circumstellar interaction (e.g. Kiewe et al. 2012). In some cases this interaction can be extremely luminous (Smith et al. 2010, 2011a). The necessary mass loss is often attributed to prior outbursts of the star as a luminous blue variable (LBV; e.g. Smith et al. 2011b) or a pulsational-pair-instability supernova (PPISN, Woosley et al. 2007), though other possibilities, e.g. common envelope (Chevalier 2012a), are sometimes invoked.

The luminosity of colliding shells is limited by their differential speeds, their masses, and the radii at which they collide. If the collision happens at too small a radius where the ejecta is still very optically thick, colliding shells become another variant of ‘‘prompt explosions’’ (§ 2). On the other hand, if the collision happens at too large a radius, the resulting transient has a longer time scale, lower luminosity, and may not emit chiefly in the optical (Chevalier & Irwin 2012b). In practice, these constraints limit the radius where the shells collide and produce a bright optical transient to roughly 10^{15} - 10^{16}

cm. A similar range of radii is obtained by multiplying typical collision speeds, $\sim 5,000 \text{ km s}^{-1}$, by the duration of an ULSN, ~ 100 days.

Chevalier & Irwin (2012b) give a maximal “cooling luminosity” for colliding shells in which most of the dissipated energy goes into light (see also Smith et al. 2010, eq. 1),

$$L \lesssim 2\pi r^2 \rho v_{\text{shock}}^3 = 0.5 \frac{\dot{M}}{v_{\text{wind}}} v_{\text{shock}}^3 \quad (7)$$

where \dot{M} is the pre-explosive mass loss rate with speed v_{wind} , and v_{shock} is the shock speed of the explosive ejecta impacting that “wind”. Narrow lines in the spectra of Type II_n supernovae, including some very luminous ones (Kiewe et al. 2012), imply pre-explosion wind speeds of a few hundred to 1000 km s^{-1} . At those speeds, and given that the light curve is generated at $r \sim 10^{15} - 10^{16} \text{ cm}$, the relevant time for the mass loss is a few years before the final explosion. The velocity of the shock is $v_{\text{shock}} \approx \sqrt{2E/M}$, where E is the explosion energy of mass M . Here we normalize it to 10^9 cm s^{-1} as in Chevalier & Irwin (2012b), though it implies a very energetic explosion. The luminosity from the collision is then

$$L \approx 3.1 \times 10^{44} \frac{\dot{M}_{-1}}{v_{\text{wind},7}} v_{\text{shock},9}^3 \text{ erg s}^{-1}, \quad (8)$$

where \dot{M}_{-1} is the mass loss rate a few years before the explosion normalized to $0.1 M_{\odot}$ per year, $v_{\text{wind},7}$ is in 10^2 km s^{-1} and $v_{\text{shock},9}$ is in units of 10^4 km s^{-1} . Typical values for the outbursts that produce very bright bright Type II_n supernovae are $\dot{M}_{-1} = 1$, $v_{\text{wind},7} = 1$ to 10 , and $v_{\text{shock},9} = 0.5$ (Kiewe et al. 2012) implying peak luminosities near $5 \times 10^{43} \text{ erg s}^{-1}$. The large ejection in η -Carina in the 1840’s ejected $12 M_{\odot}$ moving at $v_{\text{wind},7}$ up to 6.5 (Smith 2008).

It is the mass of the shell into which a supernova of given energy plows that matters most (van Marle et al. 2010). We are unaware of any models other than PPISN (§ 4.2 or $10 M_{\odot}$ stars (Woosley & Heger 2015a) that eject solar masses of material just years before dying. If a generous upper limit of $10 M_{\odot}$ between 10^{15} and 10^{16} cm ($M_{10} = 1$) is adopted, $\dot{M}_{-1}/v_{\text{wind},7}$ is $\lesssim 3 M_{10} R_{16}^{-1}$ where R_{16} is the outer edge of the interaction region in 10^{16} cm units. For a shock speed $v_{\text{shock},9} = 0.5$ and an event duration of 100 days, $R_{16} \sim 0.5$. The maximum luminosity is then $10^{45} v_{\text{shock},9}^3 M_{10} R_{16}^{-1} \text{ erg s}^{-1} \approx 3 \times 10^{44} \text{ erg s}^{-1}$. More generally the maximum luminosity is $L = 10^{45} \tau_{\text{SN},100}^{-1} M_{10} v_{\text{shock},9}^2 \text{ erg s}^{-1}$ where $\tau_{\text{SN},100}$ is the duration of the brightest part of the light curve. This limit is sufficient to accommodate all ULSN that maybe powered by collisions and is consistent with the theoretical results of van Marle et al. (2010).

It might be possible to raise this limit by invoking slightly greater shock speeds or shell masses. The former requires extremely energetic supernovae though. Accelerating a shell of $10 M_{\odot}$ to 10^9 cm s^{-1} requires an explosion energy of at least 10^{52} erg and 100% conversion efficiency. This is considerably more than neutrinos can provide and already indicates a source that is, at heart, rotationally powered. Yet it may be that having high mass loss rates removes sufficient angular momentum to

inhibit the formation of rapidly rotating iron cores. Even energetic PISN do not develop speeds of $10,000 \text{ km s}^{-1}$ in a significant part of their mass. Moreover, PISN are burning carbon radiatively in their centers the last few years of their life and, except for PPISN (§ 4.2), experience no obvious instability that would lead to the impulsive ejection of $10 M_{\odot}$.

With considerable uncertainty, we thus adopt an upper limit for colliding shells of $3 \times 10^{44} \text{ erg s}^{-1}$ and a total radiated energy of $\tau_{\text{SN}} L \sim 3 \times 10^{51} \text{ erg}$. For bare helium cores which are not PPISN and clearly not LBVs, the values are likely to be much smaller because of the smaller shell masses, but existing models, do not allow a specific estimate.

4.2. Pulsational-pair instability supernovae

The most luminous colliding shell models with definite predictions for their luminosity are PPISN (Woosley et al. 2007; Yoshida et al. 2016). For a narrow range of masses corresponding to stars with $50 - 55 M_{\odot}$ helium cores, a supergiant star, red or blue, will eject its hydrogen envelope at speeds $\sim 1000 \text{ km s}^{-1}$, and a year or so later eject one or more very energetic shells that smash into it (Woosley & Heger 2015b). The source of the energy is the thermonuclear burning of carbon and oxygen. For lighter helium cores, low energy shells are ejected in rapid succession before the envelope has expanded to 10^{15} cm . The collision energy is adiabatically degraded and the resulting supernova is not especially luminous (Woosley 2016, in prep.). For heavier cores, the pulses are too infrequent and produce collisions outside of 10^{16} cm that last much longer than one hundred days.

In the narrow helium-core mass range of $50 - 55 M_{\odot}$ though, one or more pulses occurring a year or so after the one that ejects the envelope, eject additional shells carrying a energy of up to $1 \times 10^{51} \text{ erg}$ (Woosley & Heger 2015b). Radiating all this energy over a 10^7 s interval gives a luminosity that can approach $10^{44} \text{ erg s}^{-1}$ (Woosley et al. 2007).

For helium cores lacking any hydrogen envelope the luminosities are less because of the lack of a massive low velocity reservoir to turn kinetic energy into light. Typical peak luminosities for Type I PPISN are thus near $3 \times 10^{43} \text{ erg s}^{-1}$, and the light curve can be more highly structured (Woosley & Heger 2015b).

5. MAGNETARS

With some tuning, the energy deposited by a young magnetar in the ejecta of a supernova can significantly brighten its light curve (Maeda et al. 2007; Woosley 2010; Kasen & Bildsten 2010). The model has been successfully applied to numerous observations of Type Ic ULSN (e.g. Inserra et al. 2013; Nicholl et al. 2013; Howell et al. 2013) and magnetars seem a natural consequence of collapse of rapidly rotating cores (e.g. Mösta et al. 2015).

The rotational kinetic energy of a magnetar with a period $P_{\text{ms}} = P/\text{ms}$ is approximately $E_{\text{m}} \approx 2 \times 10^{52} P_{\text{ms}}^{-2} \text{ erg}$, where $E_{\text{m,max}} \approx 4 \times 10^{52} \text{ erg}$ is the rotational energy for an initial period of $\sim 0.7 \text{ ms}$. Usually this period is restricted to $> 1 \text{ ms}$, because of rotational instabilities that lead to copious gravitational radiation. However, Metzger et al. (2015) have recently discussed the possibility that the limiting rotational kinetic energy could

exceed 10^{53} erg, depending on the neutron star mass and the equation of state and here we adopt that value as an upper bound. This energy reservoir can be tapped through vacuum dipole emission, which is approximately $E_m/t_m \approx 10^{49} B_{15}^2 P_{ms}^{-4}$ erg s^{-1} , where $B_{15} = B/10^{15}$ G is the dipole field strength at the equator, and $t_m = 2 \times 10^3 P_{ms}^2 B_{15}^{-2}$ s is the magnetar spin-down timescale. A magnetic dipole moment $B(10\text{km})^3$ is adopted, and an angle of $\pi/6$ between the magnetic and rotational axes has been assumed. Combining these relations, one obtains the temporal evolution of the rotational energy and magnetar luminosity as $E_m(t) = E_{m,0} t_m / (t_m + t)$ and $L_m(t) = E_{m,0} t_m / (t_m + t)^2$.

The peak luminosity can be estimated using the diffusion equation and ignoring the radiative losses in the first law of thermodynamics (Kasen & Bildsten 2010):

$$L_p = \frac{E_{m,0}}{t_d} \left[\xi \ln\left(1 + \frac{1}{\xi}\right) - \frac{\xi}{1 + \xi} \right], \quad (9)$$

where $\xi = t_m/t_d$ is the ratio of spin-down to effective diffusion timescales. The term inside square brackets has a maximum at $\xi \approx 1/2$, obtained by solving $d(L_p t_d / E_{m,0}) / d\xi = 0$. This implies an optimal field strength for maximizing the peak luminosity is:

$$B_{15} \Big|_{L_{p,\max}} \simeq 66 P_{ms,0} t_d^{-1/2}. \quad (10)$$

That is, for a given combination of $P_{ms,0}$ and ejecta parameters - M_{ej} , E_{sn} , κ , the brightest possible peak luminosity is obtained for this field strength.

The maximum peak luminosity is then $L_{p,\max} \simeq E_m/10t_m$. For the limiting initial spin of $P_{ms,0} = 0.7\text{ms}$ the corresponding field strength is $B \approx 4 \times 10^{13}$ G (for $\kappa = 0.1 \text{ cm}^2 \text{ g}^{-1}$, $M_{ej} = 3.5 M_\odot$ and $E_{SN} = 1.2 \times 10^{51}$ erg), and the limiting peak luminosity is $L_{p,\max} \approx 2 \times 10^{46}$ erg s^{-1} . Here $E_m \gg E_{SN}$, therefore unless one invokes even lower κ , M_{ej} and much larger E_m , any transient with brighter observed luminosity will be hard to explain by the magnetar model (Fig. 2).

Using a version of Arnett’s Rule (Inserra et al. 2013, e.g.), $L_m(t_p) = L_p$, the time for L_p is $t_p = (E_m t_m L_p^{-1})^{1/2} - t_m$. For the maximal luminosity, the corresponding peak time is then $t_{p,\max} \simeq 2.2t_m$. This can be used to estimate the limiting radiated energy in the same way as in eq. (6) to find that:

$$E_{\text{rad,max}} \simeq 0.4 E_{m,0}. \quad (11)$$

Any observation with a total radiated energy of $E_{\text{rad}} > 4 \times 10^{52}$ erg will be nearly impossible to explain by the magnetar model. A more conventional value and one that fits ASASSN-15lh (Fig. 2), is 2×10^{52} erg. This is within a factor of two of the limiting magnetar kinetic energy inferred for gamma-ray bursts by Mazzali et al. (2014).

To illustrate these limits, a series of magnetar-powered models based upon exploding CO cores (from Sukhbold & Woosley 2014) was calculated to find a best fit to the light curve of ASASSN-15lh. In each case, soon after bounce, the magnetar deposited its energy in the inner ejecta at a rate given by the vacuum dipole spin-down rate. The top panel of Fig. 2 shows the best fitting model, which employs a magnetar with an initial period of 0.7

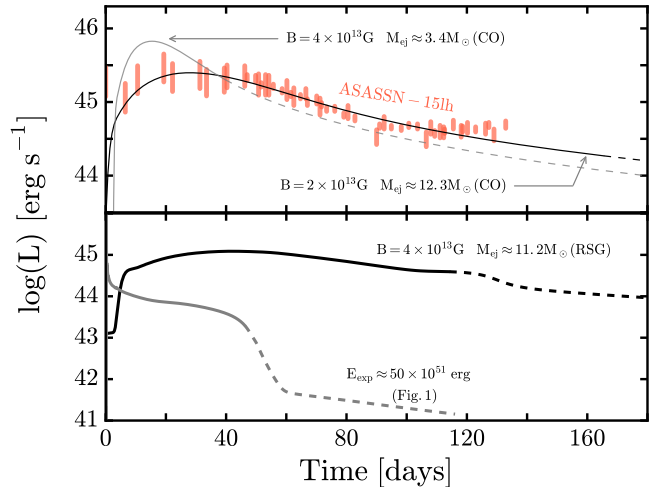


FIG. 2.— Top: The luminous transient ASASSN-15lh compared with a magnetar model in which the initial rotational energy was 5×10^{52} erg. Similar magnetars embedded in a less ejecta will give slightly brighter light curves. Bottom: The same magnetar used in the top panel for fitting ASASSN-15lh is embedded in the ejecta of a massive red supergiant progenitor. The light curve is dimmer than the Type I case, but substantially brighter than the prompt explosion case shown in Fig. 1. The dashed curve marks the transition to nebular phase.

ms and magnetic field strength of 2×10^{13} G, illuminating the ejecta in the explosion of a $14 M_\odot$ CO core ($M_{ej} \approx 11.2 M_\odot$).

These magnetar parameters agree well with the previously published fits, but the ejecta masses are different. An ejecta mass of $15 M_\odot$ was obtained by Dai et al. (2016), as they used simple semi-analytical models, which ignored all dynamical effects and deviate from hydrodynamic calculations most when $E_m \gg E_{sn}$. An ejecta mass of only $3 M_\odot$ was used in Metzger et al. (2015), as they applied the same simple semi-analytical model for the early release of the data spanning only ~ 60 days. That fit would not work for the later data shown in Fig. 2, and the ejecta would become optically thin at an early time. Bersten et al. (2016) limited their models to small He-cores ($8 M_\odot$), and their model does not fit the broad peak of ASASSN-15lh well.

Magnetars can also illuminate bright, long lasting Type II supernovae. The bottom panel of Fig. 2, shows the same magnetar that was applied for the fit to ASASSN-15lh, now embedded inside the remnant of a $15 M_\odot$ red supergiant progenitor. Because the ejecta mass is much larger, the light curve is fainter and much broader. The ejecta stays optically thick for nearly 4 months. Much as radioactive decay extends the plateau duration by causing ionization, magnetar-deposited energy also significantly extends the optically thick period.

6. CONCLUSIONS

Table 1 summarizes the maximum luminosity and total luminous energy for the models considered. Given the various approximations made, the numbers are probably accurate to a factor of two in most cases except for shell “collisions” where definitive models are lacking (§ 4.1). In all but the magnetar-powered models, the peak luminosities are a few times 10^{44} erg s^{-1} and peak integrated powers are near 10^{51} erg. This is gratifying since most “superluminous supernovae” are within those

TABLE 1
LIMITING PEAK LUMINOSITIES AND
RADIATED ENERGIES

	model	L_p [erg s ⁻¹]	E_{rad} [erg]
Type II	prompt	1×10^{44}	3×10^{50}
	PISN	5×10^{43}	1×10^{51}
	collisions	3×10^{44}	3×10^{51}
	PPISN	1×10^{44}	1×10^{51}
	magnetar	1×10^{45}	9×10^{51}
Type I	PISN	2×10^{44}	3×10^{51}
	PPISN	3×10^{43}	1×10^{51}
	magnetar	2×10^{46}	4×10^{52}

bounds (e.g. Nicholl et al. 2015).

For point-like explosions, which includes PISN of Type II, the prompt energy injection is typically degraded by a factor of ~ 100 by adiabatic expansion, so even obtaining 10^{51} erg of light requires an explosion that strains the limits of both neutron star binding energy (core-collapse supernovae) and thermonuclear energy (PISN). The upper bound for PISN-Type I is also well determined by both analytic scaling rules and numerical models.

For supernovae whose light comes from colliding shells, the constraints are less accurate due to lack of knowledge about the masses of the shells involved and the supernova explosion energies in cases where large impulsive mass loss occurs just before the star dies. The limit in the table assumes shock speeds less than 5000 km s^{-1} and shell masses less than $10 M_{\odot}$. Estimates for PPISN are more precise because the mass of the helium core needed to make luminous optical supernovae is highly constrained.

In order that the duration of the pulses be years and not months or centuries, the helium core mass need to be in the range $50 - 55 M_{\odot}$ and that restricts the energy of the secondary pulses and supernova.

Magnetars are a special case. The limits come from using a simple dipole formula in a situation where it has not been observationally tested and assuming what some would regard as a high limiting rotational energy for neutron stars. Rotation can tap an energy reservoir almost as great as the binding energy of the neutron star and deposit it over an arbitrarily long time scale - depending on the choice of magnetic field strength. Thus the optical efficiency for converting rotational energy to light can be (forced to be) very high.

It is interesting though that the upper bounds for magnetar-powered light curves are so high. This implies a possible observable diagnostic. Supernovae that substantially exceed $3 \times 10^{44} \text{ erg s}^{-1}$ for an extended period and which have total luminous powers far above $3 \times 10^{51} \text{ erg}$ should be considered strong candidates for containing an embedded magnetar. Similarly, ‘‘supernovae’’ that exceed the generous limits for magnetar power given in Table 1 may not be supernovae at all.

ASASSN-15lh (Dong et al. 2016) is an interesting case in this regard. Fig. 2 shows that it can, barely, be accommodated by a magnetar model and Table 1 says it must be a magnetar, if it is a supernova (Brown 2015).

7. ACKNOWLEDGEMENTS

We thank Alex Heger for his contributions in developing the KEPLER code and Chris Kochanek, Iair Arcavi, Matt Nicholl and Todd Thompson for useful comments. This work was supported by NASA (NNX14AH34G).

REFERENCES

- Arnett, W. D. 1979, *ApJ*, 230, L37
- Bersten, M. C., Benvenuto, O. G., Orellana, M., & Nomoto, K. 2016, arXiv:1601.01021
- Brown, P. J. 2015, *The Astronomer’s Telegram*, 8086
- Chatzopoulos, E., Wheeler, J. C., Vinko, J., Horvath, Z. L., & Nagy, A. 2013, *ApJ*, 773, 76
- Chen, K.-J., Heger, A., Woosley, S., et al. 2014c, *ApJ*, 790, 162
- Chevalier, R. A. 2012, *ApJ*, 752, L2
- Chevalier, R. A., & Irwin, C. M. 2012, *ApJ*, 747, L17
- Dai, Z. G., Wang, S. Q., Wang, J. S., Wang, L. J., & Yu, Y. W. 2016, *ApJ*, 817, 132
- Dong, S., Shappee, B. J., Prieto, J. L., et al. 2016, *Science*, 351, 257
- Ertl, T., Janka, H.-T., Woosley, S. E., Sukhbold, T., & Ugliano, M. 2016, *ApJ*, 818, 124
- Fryer, C. L., & Kalogera, V. 2001, *ApJ*, 554, 548
- Fuller, G. M., Woosley, S. E., & Weaver, T. A. 1986, *ApJ*, 307, 675
- Gal-Yam, A. 2012, *Science*, 337, 927
- Heger, A., & Woosley, S. E. 2002, *ApJ*, 567, 532
- Howell, D. A., Kasen, D., Lidman, C., et al. 2013, *ApJ*, 779, 98
- Insera, C., Smartt, S. J., Jerkstrand, A., et al. 2013, *ApJ*, 770, 128
- Kasen, D., & Woosley, S. E. 2009, *ApJ*, 703, 2205
- Kasen, D., & Bildsten, L. 2010, *ApJ*, 717, 245
- Kasen, D., Woosley, S. E., & Heger, A. 2011, *ApJ*, 734, 102
- Kozyreva, A., & Blinnikov, S. 2015, *MNRAS*, 454, 4357
- Maeda, K., Tanaka, M., Nomoto, K., et al. 2007, *ApJ*, 666, 1069
- Mazzali, P. A., McFadyen, A. I., Woosley, S. E., Pian, E., & Tanaka, M. 2014, *MNRAS*, 443, 67
- Metzger, B. D., Margalit, B., Kasen, D., & Quataert, E. 2015, *MNRAS*, 454, 3311
- Mösta, P., Ott, C. D., Radice, D., et al. 2015, *Nature*, 528, 376
- Nicholl, M., Smartt, S. J., Jerkstrand, A., et al. 2013, *Nature*, 502, 346
- Nicholl, M., Smartt, S. J., Jerkstrand, A., et al. 2015, *MNRAS*, 452, 3869
- Pejcha, O., & Thompson, T. A. 2015, *ApJ*, 801, 90
- Popov, D. V. 1993, *ApJ*, 414, 712
- Quimby, R. M., Kulkarni, S. R., Kasliwal, M. M., et al. 2011, *Nature*, 474, 487
- Kiewe, M., Gal-Yam, A., Arcavi, I., et al. 2012, *ApJ*, 744, 10
- Scannapieco, E., Madau, P., Woosley, S., Heger, A., & Ferrara, A. 2005, *ApJ*, 633, 1031
- Smith, N. 2008, *Nature*, 455, 201
- Smith, N., Chornock, R., Silverman, J. M., Filippenko, A. V., & Foley, R. J. 2010, *ApJ*, 709, 856
- Smith, N., Li, W., Miller, A. A., et al. 2011, *ApJ*, 732, 63
- Smith, N., Li, W., Silverman, J. M., Ganeshalingam, M., & Filippenko, A. V. 2011, *MNRAS*, 415, 773
- Sukhbold, T., & Woosley, S. E. 2014, *ApJ*, 783, 10
- Sukhbold, T., Ertl, T., Woosley, S. E., Brown, J. M., & Janka, H.-T. 2015, arXiv:1510.04643
- Ugliano, M., Janka, H.-T., Marek, A., & Arcones, A. 2012, *ApJ*, 757, 69
- van Marle, A. J., Smith, N., Owocki, S. P., & van Veelen, B. 2010, *MNRAS*, 407, 2305
- Weaver, T. A., Zimmerman, G. B., & Woosley, S. E. 1978, *ApJ*, 225, 1021
- Woosley, S. E., Heger, A., & Weaver, T. A. 2002, *Reviews of Modern Physics*, 74, 1015
- Woosley, S. E., Blinnikov, S., & Heger, A. 2007, *Nature*, 450, 390
- Woosley, S. E. 2010, *ApJ*, 719, L204
- Woosley, S. E., & Heger, A. 2015, *ApJ*, 810, 34
- Woosley, S. E., & Heger, A. 2015, *Very Massive Stars in the Local Universe*, 412, 199

